Impact of protein identity on tumor-associated antigen uptake into infiltrating immune cells: A comparison of different fluorescent proteins as model antigens

Rulan Yi[1], Emily Chen[2], Edward W Roberts[3], Matthew F Krummel[2*], Nina K Serwas[2*]

[1]MCB Undergraduate Program, University of California, Berkeley, CA, USA

[2]Department of Pathology, University of California, San Francisco, CA, USA

[3] Cancer Research UK Beatson Institute, Glasgow, UK

*Corresponding authors:

E-mail: matthew.krummel@ucsf.edu (MFK), nina.serwas@ucsf.edu (NKS)

Abstract

Effective immune responses depend on efficient antigen uptake in the periphery, transport of those antigens to, and presentation in draining lymph nodes (LNs). These processes have been studied intensively using stable fluorescent proteins (FPs) as model antigens. To date, ZsGreen is the only FP that can be tracked efficiently towards LNs, hence, it is difficult to compare studies using alternated tracking proteins.

Here, we systematically compared six different FPs. We included ZsGreen, ZsYellow, DsRed, AsRed, mCherry, and mRFP based on sequence homology and/or origin species, and generated FP-expressing tumor cell lines. Stability of fluorescent signal was assessed *in vitro*

19 over time, across different pH environments, and *in vivo* through FP antigen uptake and transfer
20 to immune cells isolated from tumors and tumor-draining LNs.

21 ZsGreen could be detected in high percentages of all analyzed tumor-infiltrating immune
22 cells, with highest amounts in tumor-associated macrophages (TAMs) and type 2 conventional
23 dendritic cells (cDC2s). ZsYellow, AsRed, and DsRed followed a similar pattern, but
24 percentages of FP-containing immune cells in the tumor were lower than for ZsGreen.
25 Strikingly, mRFP and mCherry demonstrated a 'non-canonical' antigen uptake pattern where
26 percentages of FP-positive tumor-infiltrating immune cells were highest for cDC1s not TAMs
27 and cDC2s despite comparable stabilities and localization of all FPs. Analysis of antigen-
28 containing cells in the LN was hindered by intracellular degradation of FPs. Only ZsGreen could
29 be efficiently tracked to the LN, though some signal was measurable for ZsYellow and DsRed.

30 In summary, we find that detection of antigen uptake and distribution is subject to
31 variabilities related to fluorophore nature. Future experiments need to consider that these
32 processes might be impacted by protein expression, stability, or other unknown factors. Thus,
33 our data sheds light on potential under-appreciated mechanisms regulating antigen transfer and
34 highlights potential uses and necessary caveats to interpretation based on FP use.

Introduction

For a successful tumor immune response, the proper uptake and presentation of tumor-associated antigens (TAAs) by antigen presenting cells (APCs), such as dendritic cells (DCs), is essential. As such, antigens from peripheral tissues need to be taken up by phagocytic APCs which mature, upregulate costimulatory molecules, and present these antigens as processed peptides on MHC complexes. During this process, APCs traffic from the peripheral tissue where the tumor is located to the tumor-draining lymph node (tdLN). There, the APCs can interact with T and B cells to generate an effective long-term response [1,2]. The interaction of the TAA-peptide:MHC complex and its accessory proteins with receptors on T and B cells determines downstream immune responses such as cell activation and differentiation. Exactly how TAAs are taken up and brought to the LN for presentation is not fully understood.

Previous studies showed that type 1 DCs (cDC1s) are essential for the transport of TAAs to the lymph node, and that this transport is dependent on C-C chemokine receptor 7 (Ccr7) [3,4]. Upon entry into the LN, migratory DCs can transfer antigens to other lymph node resident DCs as membrane encapsulated vesicles through direct cell-cell contact [5]. The choice of the receiving DCs may then dictate the downstream immune responses generated through subsequent T cell interaction causing activation, proliferation, memory induction, and/or effector responses in the T cell [5]. Previous studies that analyzed the process of antigen uptake, presentation, and transfer have used fluorescent proteins (FPs) such as mCherry, green fluorescent protein (GFP), yellow fluorescent protein (YFP), tdTomato, and ZsGreen as model antigens [3–5]. FPs used in these studies seemed to have different stabilities since only ZsGreen was substantially detected in resident dendritic cells. Importantly, other tumor antigens can be tracked in those resident DCs as well, confirming that ZsGreen presence was not an artifact, but

58 faithfully reported on transport [5]. It is not clear why other FPs cannot be transported to the
59 same extend to the tdLNs and whether certain properties of FPs alter antigen uptake and
60 distribution or simply degrade more rapidly than others *en route* to the LN.

61 A wide range of FPs exists that are frequently used in imaging and tracking experiments.
62 These FPs have varying brightness and stabilities that may potentially impact the outcome of
63 antigen uptake, transfer, and presentation. Brightness is defined as extinction coefficient times
64 quantum yield at pH 7.4 [6] and can range from dim proteins, such as AsRed derived from
65 *Anemonia sulcate*, with a brightness index of 2.81 [7], to bright proteins with indices of 90
66 (tdTomato) [6]. Stability is dependent on the specific environment in which the FP resides at the
67 time of analysis [6]. In this study we tested antigen stability *in vitro* and *in vivo* for six different
68 FPs with a range of brightness indexes between 2.81 and 49. We tracked their stabilities during
69 uptake and intracellular storage in tumor-infiltrating immune cells and after transport to the
70 tdLNs. The combined results offer a comprehensive overview of the properties of the chosen
71 FPs with regards for their usefulness in assays tracking antigen uptake and transfer. This work
72 will facilitate the choice of FPs in studies that will use two or more fluorophores in parallel.

73

Material and methods

Alignment

Amino acid sequences of all fluorescent proteins used were gathered via FPbase [7], then aligned via Basic Local Alignment Search Tool (BLAST) [8]. Percent similarity to ZsGreen and DsRed were determined using the global align tool.

Mice

Mice were housed and bred under specific pathogen free conditions at the University of California, San Francisco Laboratory Animal Research Center and all experiments conformed to ethical principles and guidelines approved by the UCSF Institutional Animal Care and Use Committee. C57BL/6 mice were purchased from Jackson Laboratory or bred in-house. Male mice between 8-12 weeks of age were used.

Cell lines

Vectors containing target fluorescent genes ZsGreen, ZsYellow, DsRed, AsRed, mCherry, and mRFP (Takara Bio), were either transfected into B16-F10 cells using the calcium chloride precipitation method (all FPs except ZsGreen), or retrovirally transduced into B16F10 cells (ZsGreen). Transformed cells were then harvested, washed, and repeatedly sorted through fluorescent activated cell sorting (FACS) on a BD FACSAria™ to select for stable fluorescent positive populations. Sorted cells were then collected, frozen and/or propagated for use in future experiments. Cells were cultured at 37°C with 5% CO_2 in DMEM (GIBCO) plus 10% heat-inactivated FCS with penicillin, streptomycin, and L-glutamate on tissue-culture treated plastic plates and split every other day.

Fluorescence stability assay

FP-expressing B16-F10 cells were harvested with trypsin, counted, and washed in ice cold PBS. Then, cells were homogenized with mechanical force generated through repeated passage of cells through a 22-gauge needle in hypotonic lysis buffer (20mM HEPES buffer, 2mM EGTA, 2mM MgCl2). Lysates were transferred to 96-well black microplates suitable for fluorescent based assays (Invitrogen). Each well contained lysates of 1 Mio cells. pH was adjusted with NaOH or HCl, controlled with a pH-meter before the assay, and controlled with pH-indicator strips on the lysates after the experiment to ensure that the pH was stable overtime. For each different fluorophore and pH condition, three technical replicates were performed. Data was collected over varying time points using a microplate reader (SpectraMax) and incubated at 37°C or 4C, respectively. Analysis of whole cells was done similarly in separate plates. The experiment was done in biological triplicates.

Ectopic tumor injections

B16-F10 cells expressing the respective FP were grown to 80% confluency, then harvested, washed, and counted. Cells were resuspended in a suitable amount of PBS and mixed at a 1:1 (v:v) ratio with growth factor reduced Matrigel Matrix (BD Biosciences). A final injection volume of 100ul containing 400k cells was injected subcutaneously on the flanks of mice.

Harvest, collection of data, and analysis

Tumors, inguinal and axillary lymph nodes were harvested 2 weeks after injection. After digestion with DNAse, Collagenase I and Collagenase IV, washing, and counting, 10 million cells per FP were stained with fixable Live/Dead Zombie (BioLegend) and respective antibodies:

117 MHCII-BV421, F4/80-BV510, CD11b-BV605, CD11c-BV650, Ly6C-BV711, CD45R-BV785,
118 CD90.2-BV785, Ly6G-BV785, NK1.1-BV785, CD8alpha-PerCPCy5.5, CD103-APC, CD45-
119 AF700, CD24-PECy7 (Biolegend, eBioscience).

120 Flow cytometry was performed on a BD LSR Fortessa instrument at the ImmunoX Flow
121 Cytometry CoLab. Analysis of flow cytometry data was done using FlowJo (Treestar) software,
122 and graphs and figures were produced with GraphPad Prism software. All experiments were
123 done in triplicates.

124 Fluorescence microscopy

125 Cells from each respective fluorescent cell line were thawed and cultured. 50,000 cells
126 were seeded in a poly-L-lysine coated 8-well chambered coverslip and let rest overnight. For
127 live cell imaging, a Leica SP5 laser scanning confocal microscope with an incubation chamber
128 and a 20X oil objective was used to visualize adherent cells expressing respectively ZsGreen,
129 ZsYellow, AsRed, DsRed, mRFP, and mCherry. The experiment was done in triplicates.

130 # Results and discussion

131 ## Characteristics of selected fluorescent protein

132 We compared five different fluorescent proteins (FPs) for antigen uptake and transfer
133 characteristics to ZsGreen. ZsGreen is to date the only fluorophore that can be efficiently
134 tracked from expressing tumors to lymph node resident dendritic cells. Our selection (Table 1)
135 was based on species origin (ZsYellow), brightness of the fluorophore (DsRed), sequence
136 homology (mCherry, mRFP) and availability of corresponding biochemical tools (AsRed,
137 mRFP, mCherry). ZsGreen, is derived from corals of the *Zoanthus sp*, and has been shown to
138 have high stability in various chemical environments [9]. Its brightness index is 22.43 [7].
139 ZsYellow is a stable protein purified from the same species as ZsGreen, and is excited at a
140 wavelength around 528 nm with a brightness index of 13 [7,9]. DsRed is derived from
141 *Discosoma sp* [10], excited by a wavelength of 558 nm, and has a brightness index of 49.3 [7].
142 Naturally occurring FPs such as DsRed have been modified to achieve proteins with optimized
143 brightness and stability properties such as mRFP and mCherry, with brightness indices of 12.5
144 and 15.84 respectively [7]. In addition, these modified proteins exist as monomers in contrast to
145 the tetrameric nature of ZsGreen and DsRed [7]. AsRed has the lowest brightness in our
146 collection (2.81) and is expressed in the coral species *Anemonia sulcate* [6,7,10].

147 FP-encoding vectors were transfected or transduced into B16-F10 cell lines. Transformed
148 cells with the highest signal for the respective FP were repeatedly sorted with a 5 %- cut-off
149 using fluorescence activated cell sorting (FACS) (Figs 1A and B). All generated cell lines
150 reached high FP positivity with a 2-3 log fluorescent intensity difference over un-transformed
151 cells (Figs 1A and B). Despite repeated and stringent selection for FP-positivity, both ZsYellow-

152 and mCherry-transfected B16-F10 cells kept a substantial amount of non-fluorescent cells in
153 their cultures (Fig 1B). This might be due to non-stable integration or epigenetic silencing of the
154 transgene. In subsequent analyses we considered this bimodal distribution as a potential factor
155 for differences in antigen uptake or distribution. Previous work has shown that differential
156 subcellular localization has an effect on antigen uptake and distribution into compartments of the
157 immune system [11]. All generated cell lines had their respective FPs evenly distributed in the
158 cytoplasm (S1 Fig).

159

160 **Table 1. Fluorophore properties**[7,8]

Fluorophore	Brightness	Excitation	Emission	% similarity to ZsGreen	% similarity to DsRed
AsRed	2.81	576 nm	592 nm	53.78%	61.54%
mRFP	12.5	584 nm	607 nm	56.65%	87.56%
ZsYellow	13	528 nm	539 nm	91.77%	58.87%
mCherry	15.84	587 nm	610 nm	53.53%	82.63%
ZsGreen	22.43	496 nm	506 nm	—	59.23%
DsRed	49.3	558 nm	583 nm	59.23%	—

161 Summary of used fluorophores and their respective similarity with ZsGreen and DsRed [7,8]

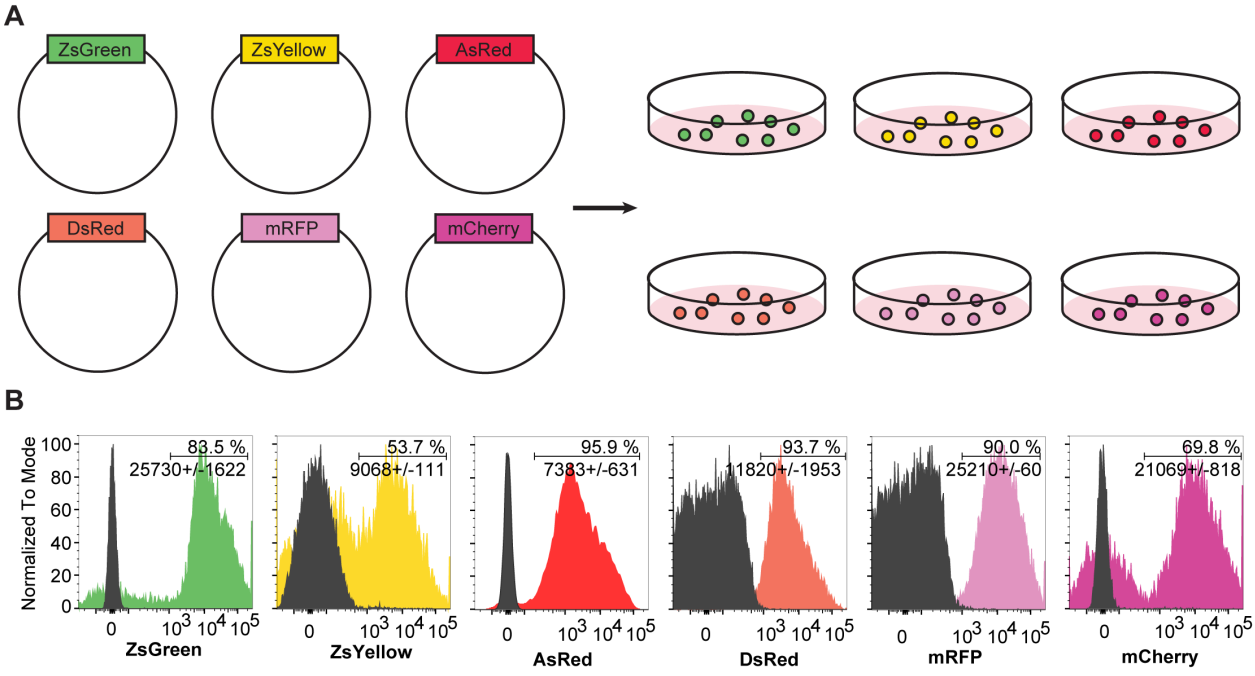

Fig 1. Generation of cell lines with respective fluorescent genes for downstream analysis.

A) Retroviral vectors expressing respective fluorescent genes ZsGreen, ZsYellow, mCherry, mRFP, DsRed, and AsRed were transfected/transduced into B16-10 cells. **B)** Fluorescence-activated cell sorting (FACS) was then used to select for FP positivity. ZsYellow and mCherry cells display a bimodal pattern despite undergoing FACS multiple times with a selection criterion for the top 5% of FP positive cells. Histograms are shown with % positive cells and average mean fluorescence intensity of the chosen fluorophore (+/- standard deviation).

170 ## Assessment of *in vitro* stability

171 The stability of fluorophores expressed in the generated cell lines was assessed in an *in*
172 *vitro* fluorescent stability assay. For this purpose, FP-expressing B16-F10 cell lines were lysed
173 in a hypotonic lysis buffer. Lysates were then kept at 37ºC to mimic the cellular environment.
174 No protease inhibitors were added. This allowed us to follow protein stability in the cytosolic
175 soup containing various proteases and other enzymes, through fluorescence intensity, over time.
176 As this assay investigates the stability of FPs, and not their individual brightness, we internally
177 normalized the brightness to timepoint 0 in neutral pH conditions. In general, ZsGreen
178 demonstrated the highest stability of all analyzed FPs, and showed only a minimal decrease in
179 fluorescent signal over the time frame of 6 hours (Fig 2A). This high stability of ZsGreen is in
180 concordance to previous published work [9]. In contrast, all other FPs showed a severe reduction
181 of signal over the first two hours (Fig 2A). Acidification of the protein lysates showed relative
182 robustness of all FPs to pH alterations (Fig 2B). The highest fluorescent intensity of all FPs
183 could be detected at neutral pH conditions which is in line with previous published analyses of
184 pH stability for fluorescent proteins [12]. Our data suggests that the impact of acidification in
185 certain intracellular compartments only plays a minimal role on FP fluorescence intensity and
186 stability. However, proteins might be degraded over time through intracellular proteases or other
187 enzymes, which was especially true for ZsYellow, AsRed, DsRed, mRFP, and mCherry.
188 ZsGreen markedly showed resistance towards degradation by proteins contained in the cellular
189 lysates which might explain its superior performance in tumor-associated antigen tracking
190 experiments. Differences between FPs other than ZsGreen in those assays seem to not be caused
191 by different fluorescence stabilities.

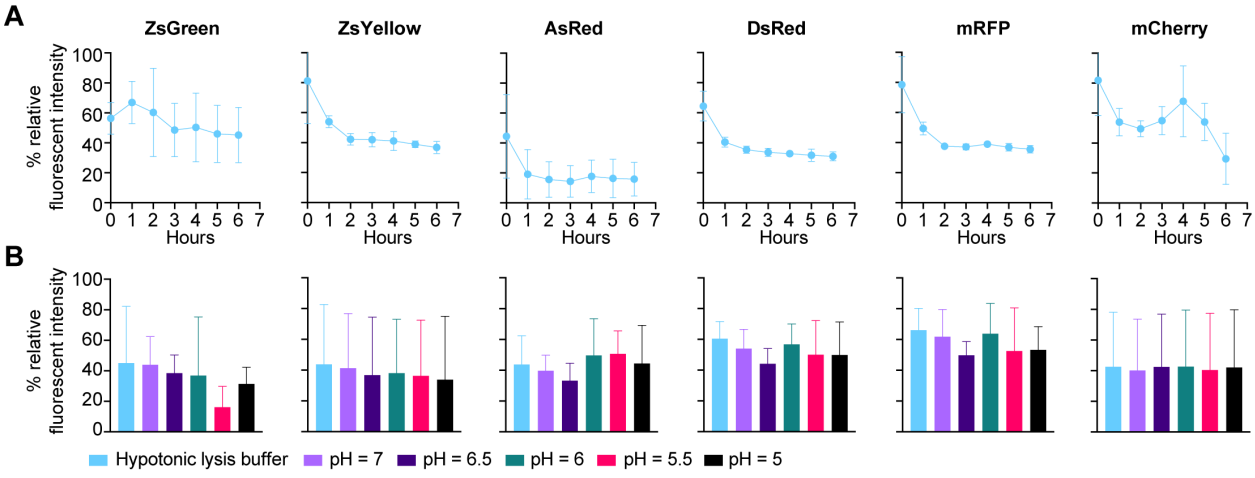

Fig 2. *In vitro* stability assay shows comparable stabilities of selected fluorophores.

Lysates of 1 million respective FP-expressing B16-F10 cells were generated in hypotonic lysis buffer and incubated at **A)** 37ºC in pH 7.4 or **B)** 37ºC in pH ranging from 5-7.4. Fluorescence intensity data was collected over time at the indicated time points (**A**) or immediately following pH treatment (**B**). Data was normalized to the maximum fluorescence intensity of each FP for every independent experiment.

200 # Tumor-associated antigen uptake varies for different FPs

201 To evaluate tumor-associated antigen (TAA) uptake of the six selected FPs, cells were
202 injected bilaterally into the flanks of B6 mice (Fig 3A). Tumors averaged a size of 1300 mm^3 for
203 all FP-containing cell lines two weeks after inocculation (Fig 3B). None of the generated FP-
204 expressing B16-F10 cell lines resulted in severe increase or reduction of tumor growth,
205 suggesting that the modification did not alter proliferation or fitness of the cells. For antigen
206 tracking analysis, only tumors of a size equal to or greater than 800 mm^3 were included.

207 We assessed distribution of FPs into different cellular populations of the tumor, namely
208 monocytes, neutrophils, tumor associated macrophages (TAMs), and DCs (Fig 4 and S2 Fig). Of
209 note, infiltrating immune cell composition were similar for all injected tumors (S3 Fig). Among
210 the selected FPs, percentages of FP-containing immune cells were highest in tumors expressing
211 ZsGreen. Interestingly, we identified two distinct antigen uptake pattern: The 'classical' pattern
212 showed highest percentages of FP-containing cells for cDC2s, TAM1s, and TAM2s. ZsGreen-
213 expressing tumor cells resulted in nearly 100% of these infiltrating immune cells to contain the
214 FP. ZsYellow-, DsRed- and AsRed-expressing tumor cells resulted in less FP-positive immune
215 cells, however, cDC2s, and TAMs were still the prime samplers of tumor associated FPs. For
216 this 'classical' uptake pattern, a smaller fraction of neutrophils, monocytes, and cDC1s displayed
217 FP signal than seen for cDC2s and TAMs. The 'non-canonical' antigen uptake pattern was
218 characterized by highest proportions of FP-positive cells for cDC1s and not cDC2s or TAMs.
219 Also for this pattern, the lowest amount of transferred antigen could be seen in neutrophils and
220 monocytes. Both, mRFP- and mCherry-expressing tumors resulted in such a distinct pattern of
221 FP uptake by immune cells (Fig 4). Despite comparable brightness, mCherry resulted in overall
222 higher percentages of FP-positive tumor-infiltrating immune cells than mRFP (Fig 4).

223 Remarkably, this was true although mCherry-expressing cells were a mixture of only two thirds
224 transformed and one third WT cells (Fig 1B).

225 Next, we analyzed the average amount of FPs within each of the individual populations.
226 We used normalized delta mean fluorescence intensity to visualize how much sampled FP each
227 cell population contained in comparison to other immune cells sampling from the same
228 fluorophore. Overall patterns of relative uptake per cell (Fig 5) showed more similarity than the
229 percentages of FP- positive cells (Fig 4). For most of the tumors, cDC2s and TAMs were the
230 cells that contained most FP. The only exception from this was mRFP containing neutrophils
231 which on average contained more FP than TAM2s. Despite showing a 'non-canonical' uptake
232 pattern, cDC1s infiltrating mRFP and mCherry-expressing tumors did not contain an increased
233 amount of antigen.

234 It remains unclear what causes the increased percentage of FP-positive tumor infiltrating
235 cDC1s in mRFP and mCherry-expressing tumors. Numbers of cDC1s are not different between
236 tumors expressing FPs irrespectively of whether they cause 'classical' or 'non-canonical' antigen
237 uptake patterns (S3 Fig). Of note, whereas ZsGreen, ZsYellow, AsRed, and DsRed are proteins
238 directly isolated from distinct organism, mCherry and mRFP have been designed to better serve
239 as tools for molecular biology. Changes aimed to enhance brightness and stability, and to prevent
240 dimerization[10,13].

241

242

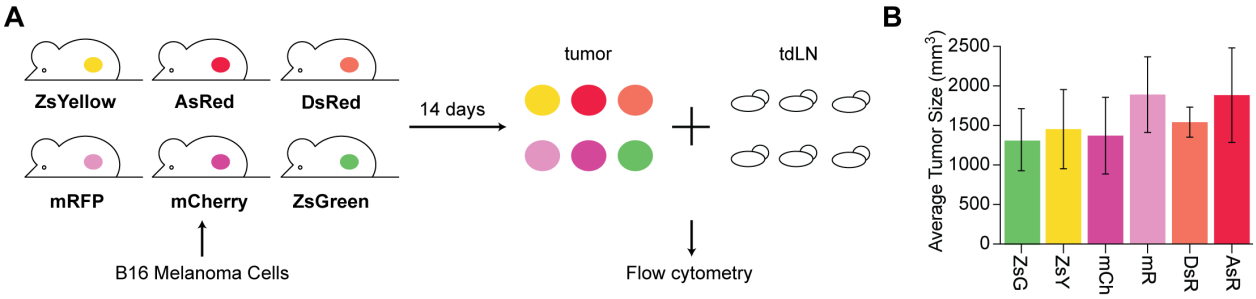

243

244 **Fig 3. Growth and harvest of respective fluorescent cell lines**

245 **A)** Fluorescent cell lines were grown, harvested, and injected subcutaneously on the
246 flanks of B6 mice. After 14 days, tumors and draining lymph nodes were harvested and
247 processed for flow cytometry. **B)** Average sizes of tumors (mm^3) at harvest are shown for all six
248 respective fluorophores. Size was controlled to ensure comparable *in vivo* growth of different
249 FP-expressing B16-F10 cell lines.

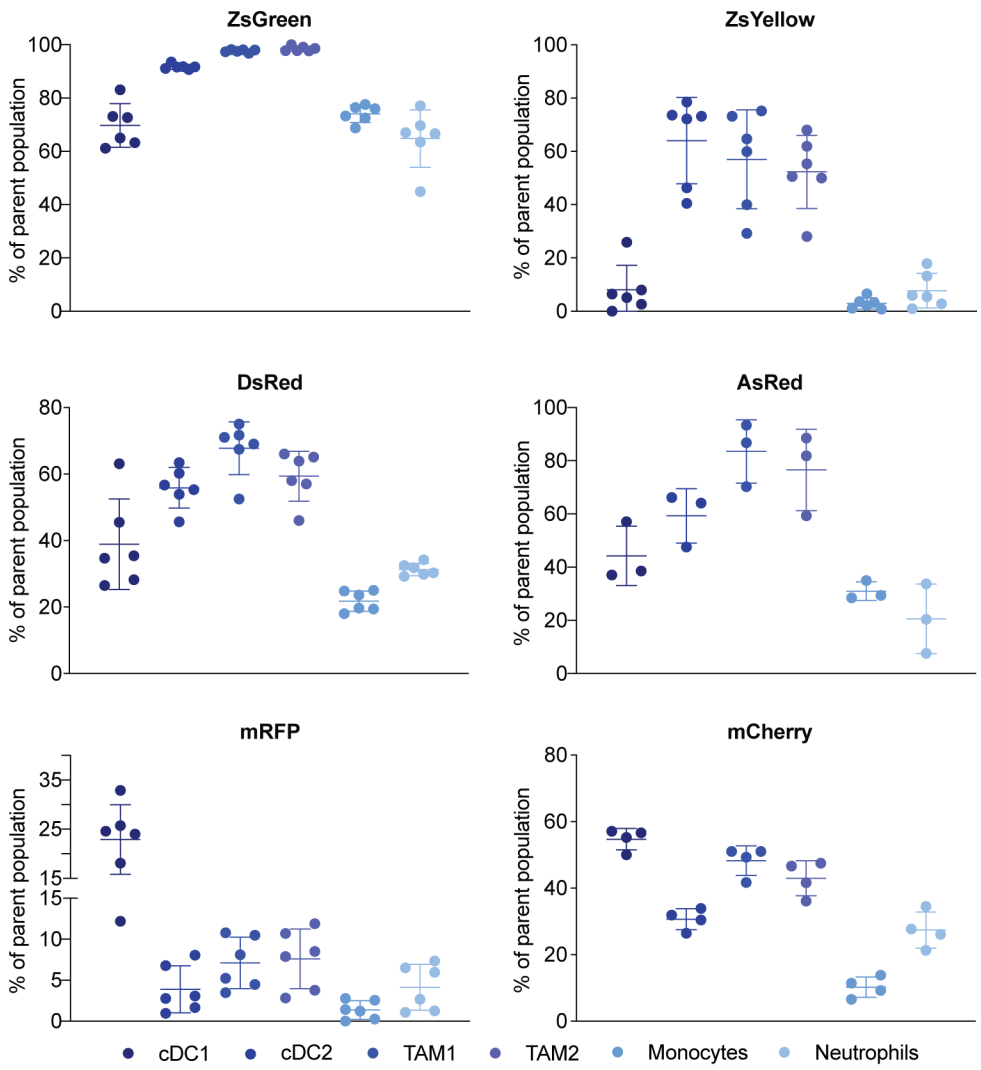

250

251 **Fig 4. TAA uptake by tumor-infiltrating immune cells identifies different patterns for**

252 **different fluorophores.**

253 Accumulation of respective fluorescent proteins in immune cells, purified from the tumor

254 microenvironment. A non-fluorescent control (B16-F10) was used to set the threshold for FP

255 positivity. One representative example of three independent experiments is shown.

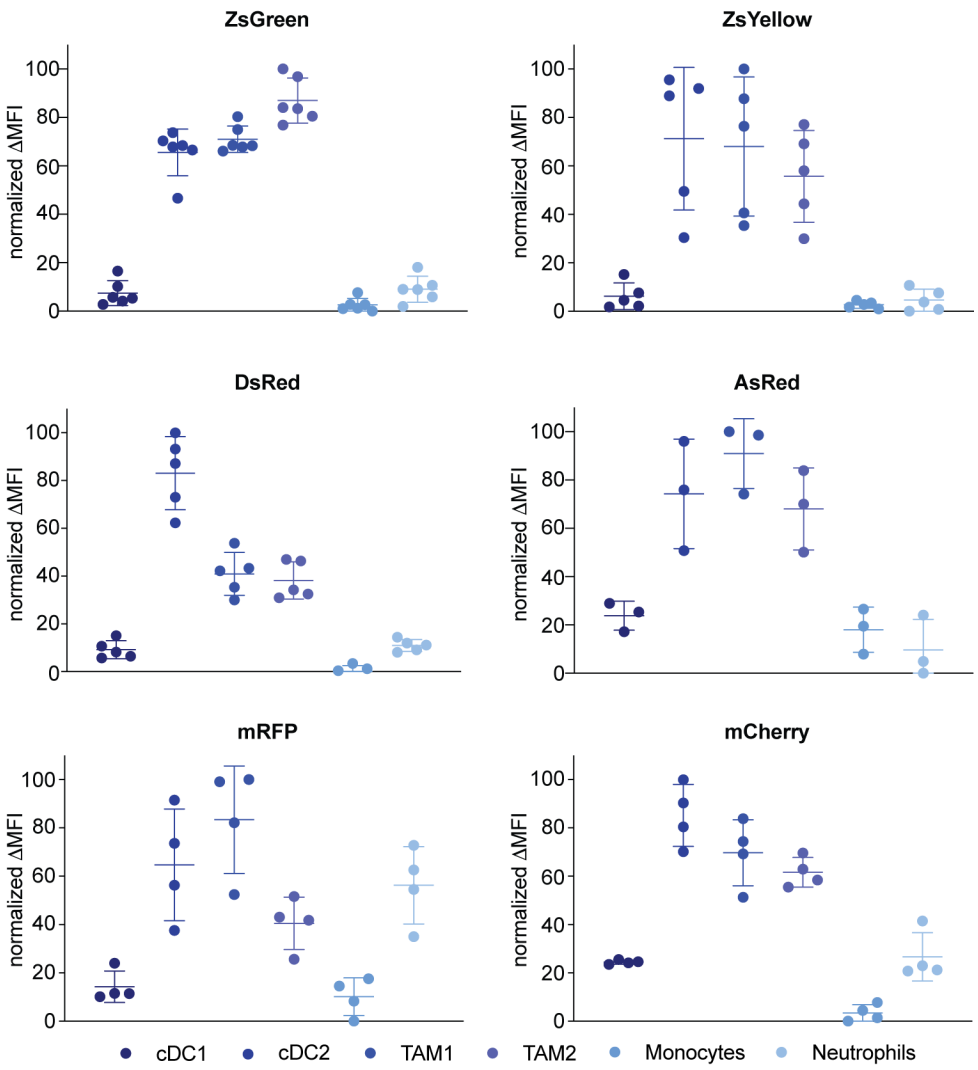

Fig 5. cDC2s and TAMs contain the most fluorescent TAAs per individual cell.

Immune cells were purified from the TME of B16 mice bearing B16 tumors with the indicated fluorophors and analyzed for relative antigen uptake. Data was normalized to the maximum delta MFI of each FP for every independent experiment.

261 ## ZsGreen, ZsYellow, and DsRed can be tracked in the tdLN

262 All investigated FPs could be detected in tumor-infiltrating immune cells to a certain
263 extend when expressed in injected B16-F10 tumor cells. Next, we wanted to determine whether
264 selected fluorophores remained intact after trafficking of the containing immune cells to tumor-
265 draining lymph nodes (tdLN). We isolated these lymph nodes and analyzed migratory and
266 resident DCs as well as monocytes by flow cytometry. Migratory DCs, monocytes, and
267 neutrophils can transport antigens to the draining LN in a Ccr7-dependent manner [3,14,15].
268 Resident DCs can receive those antigens through synaptic transfer [5].

269 Analysis of lymph nodes harvested from mice injected with B16-ZsGreen tumor cells
270 revealed FP signal in both, migratory and resident DCs, as well as in monocytes. Almost 90 %
271 of monocytes, 10-20 % of cDC1s, and up to 50 % of cDC2s had detectable ZsGreen inside them
272 (Fig 6 and S4 Fig). Other FPs showed only a limited signal suggesting that proteins could have
273 already been degraded on their way to the draining lymph node, perhaps due to shuttling of the
274 FPs into a different intracellular environment or organelle. Percentages of ZsYellow and DsRed
275 positive immune cells in respective tdLNs where with up to 20 % highest in cDC2s and
276 monocytes, but severly lower than what has been seen for ZsGreen expressing tumors.
277 Fluorescent signal in cDC1s was barely detectable. No signal could be detected in tdLN from
278 mice injected with B16 tumors expressing AsRed, mRFP and mCherry. Interestingly, previous
279 reports showed that mCherry signal could be detected in tdLNs [3]. This difference might be due
280 to different tumor models, different tumor sizes at harvest, and/or the mixture of wild type and
281 mCherry expressing cells in our cell line (Fig 1B).

282 In summary, ZsGreen was the only FP of the diverse groups of FPs tested that could be
283 tracked efficiently to the tdLN. ZsYellow and DsRed showed significantly less FP signal in

284 immune cells of the tdLN, but could still be considered as potential tools to analyze TAA

285 transfer between immune cells in tdLNs.

286

287

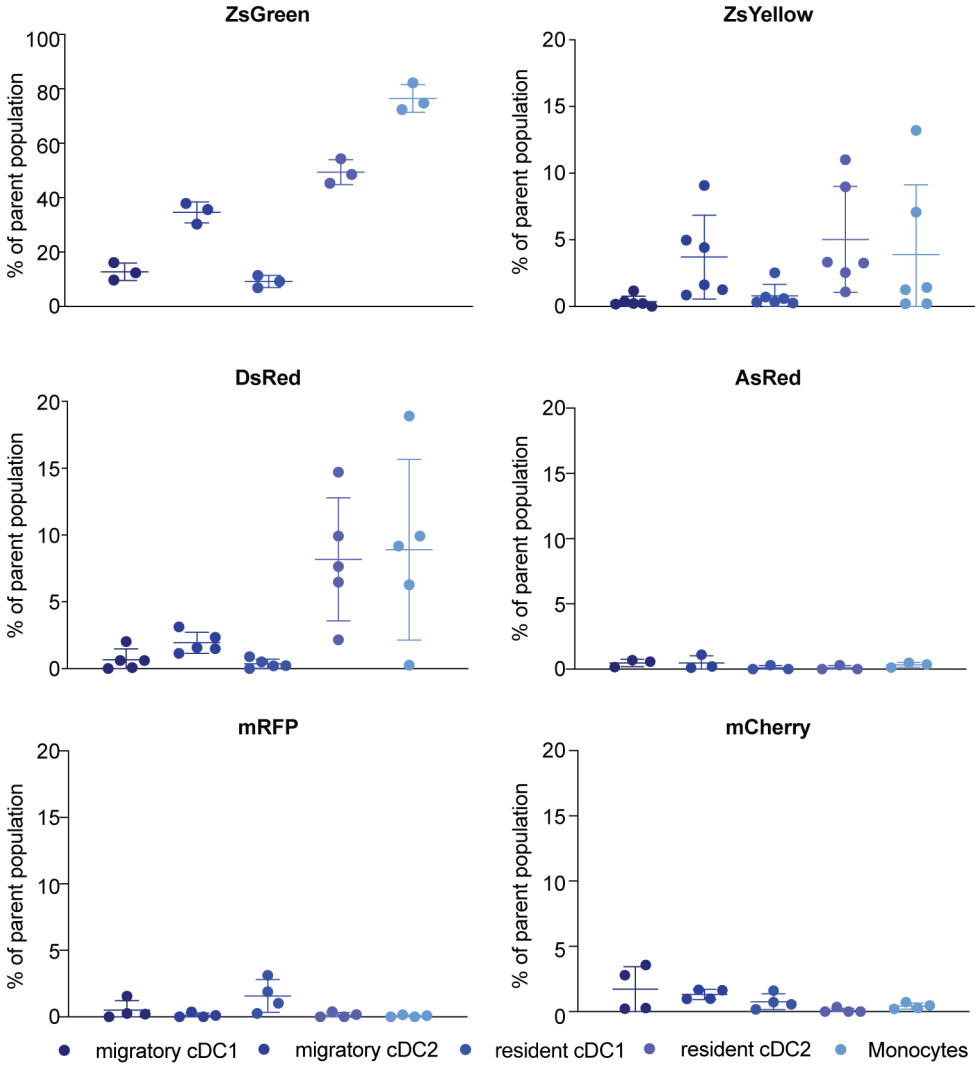

288

289 **Fig 6. Limited detection of other non-ZsGreen fluorescent proteins within immune cells of**

290 **tumor draining lymph nodes.**

291 Tumor draining (inguinal and axillary) lymph nodes were harvested, processed, and

292 analyzed through flow cytometry. Non-fluorescent control (B16-F10) was used to set the

293 threshold for FP positivity. One representative example of three independent experiments is

294 shown.

295 # Conclusion

296 In summary, we tested six FPs: ZsGreen, ZsYellow, AsRed, DsRed, mRFP, and mCherry
297 using an antigen uptake and transfer model. Despite comparable *in vitro* stabilities, those FPs
298 showed vastly different loading patterns into tumor-infiltrating immune cells. ZsGreen is the
299 only FP that can be efficiently tracked in lymph node resident DCs and remains the FP to be
300 considered best for use in antigen uptake and transfer assays. We identified ZsYellow and DsRed
301 as additional useful tools for these assays, however, tracking was not as efficient and consistent
302 as for ZsGreen and might need optimization. Additionally, we identified two distinct patterns of
303 FP-antigen loading into tumor-infiltrating immune cells. The 'classical' pattern showed
304 preferential uptake of FPs by cDC2s and TAMs, whereas the 'non-canonical' pattern revealed
305 highest antigen signal in tumor-infiltrating cDC1s. The underlying mechanisms for these distinct
306 antigen uptake patterns remain elusive. Our data suggests that analyses of antigen uptake and
307 transfer using different FPs should be carried out only after careful consideration of FP uptake
308 patterns. Potential differences might arise as a result of the nature of the chosen FPs.

309 # References

310 1. Wang Y, Xiang Y, Xin VW, Wang XW, Peng XC, Liu XQ, et al. Dendritic cell
311 biology and its role in tumor immunotherapy. Journal of Hematology and
312 Oncology. 2020;13. doi:10.1186/s13045-020-00939-6
313 2. Dersh D, Hollý J, Yewdell JW. A few good peptides: MHC class I-based cancer
314 immunosurveillance and immunoevasion. Nature Reviews Immunology. 2021;21:
315 116–128. doi:10.1038/s41577-020-0390-6
316 3. Roberts EW, Broz ML, Binnewies M, Headley MB, Nelson AE, Wolf DM, et al.
317 Critical Role for CD103+/CD141+ Dendritic Cells Bearing CCR7 for Tumor
318 Antigen Trafficking and Priming of T Cell Immunity in Melanoma. Cancer Cell.
319 2016/07/19. 2016;30: 324–336. Available:
320 http://www.ncbi.nlm.nih.gov/pubmed/27424807
321 4. Salmon H, Idoyaga J, Rahman A, Leboeuf M, Remark R, Jordan S, et al. Expansion
322 and Activation of CD103+ Dendritic Cell Progenitors at the Tumor Site Enhances
323 Tumor Responses to Therapeutic PD-L1 and BRAF Inhibition. Immunity. 2016;44:
324 924–938. doi:10.1016/j.immuni.2016.03.012
325 5. Ruhland MK, Roberts EW, Cai E, Mujal AM, Marchuk K, Beppler C, et al.
326 Visualizing Synaptic Transfer of Tumor Antigens among Dendritic Cells. Cancer
327 Cell. 2020;37: 786–799. doi:10.1016/j.ccell.2020.05.002
328 6. Shaner NC, Steinbach PA, Tsien RY. A guide to choosing fluorescent proteins.
329 Nature Methods. 2005;2: 905–909. doi:10.1038/nmeth819
330 7. Lambert TJ. FPbase: a community-editable fluorescent protein database. Nature
331 Methods. 2019;16: 277–278. doi:10.1038/s41592-019-0352-8

332 8. Altschul SF, Gish W, Miller W, Myers EW, Lipman DJ. Basic local alignment
333 search tool. Journal of Molecular Biology. 1990;215: 403–410. doi:10.1016/S0022-
334 2836(05)80360-2
335 9. Matz M V., Fradkov AF, Labas YA, Savitsky AP, Zaraisky AG, Markelov ML, et
336 al. Fluorescent proteins from nonbioluminescent Anthozoa species. Nature
337 Biotechnology. 1999;17: 969–973. doi:10.1038/13657
338 10. Shaner NC, Campbell RE, Steinbach PA, Giepmans BNG, Palmer AE, Tsien RY.
339 Improved monomeric red, orange and yellow fluorescent proteins derived from
340 Discosoma sp. red fluorescent protein. Nature Biotechnology. 2004;22: 1567–1572.
341 doi:10.1038/nbt1037
342 11. Babała N, Bovens A, De Vries E, Iglesias-Guimarais V, Ahrends T, Krummel MF,
343 et al. Subcellular localization of antigen in keratinocytes dictates delivery of CD4 þ
344 T-cell Help for the CTL response upon therapeutic DNA vaccination into the Skin.
345 Cancer Immunology Research. 2018;6: 835–847. doi:10.1158/2326-6066.CIR-17-
346 0408
347 12. Shinoda H, Shannon M, Nagai T. Fluorescent proteins for investigating biological
348 events in acidic environments. International Journal of Molecular Sciences.
349 2018;19. doi:10.3390/ijms19061548
350 13. Campbell RE, Tour O, Palmer AE, Steinbach PA, Baird GS, Zacharias DA, et al. A
351 monomeric red fluorescent protein. Proc Natl Acad Sci U S A. 2002;99: 7877–
352 7882. doi:10.1073/PNAS.082243699/SUPPL_FILE/INDEX.HTML
353 14. Abadie V, Badell E, Douillard P, Ensergueix D, Leenen PJM, Tanguy M, et al.
354 Neutrophils rapidly migrate via lymphatics after Mycobacterium bovis BCG

355 intradermal vaccination and shuttle live bacilli to the draining lymph nodes. Blood.
356 2005;106: 1843–1850. doi:10.1182/BLOOD-2005-03-1281
357 15. Özcan A, Collado-Diaz V, Egholm C, Tomura M, Gunzer M, Halin C, et al. CCR7-
358 guided neutrophil redirection to skin-draining lymph nodes regulates cutaneous
359 inflammation and infection. Science Immunology. 2022;7: 9126.
360 doi:10.1126/SCIIMMUNOL.ABI9126/SUPPL_FILE/SCIIMMUNOL.ABI9126_T
361 ABLE_S4.ZIP
362
363

Supporting Information

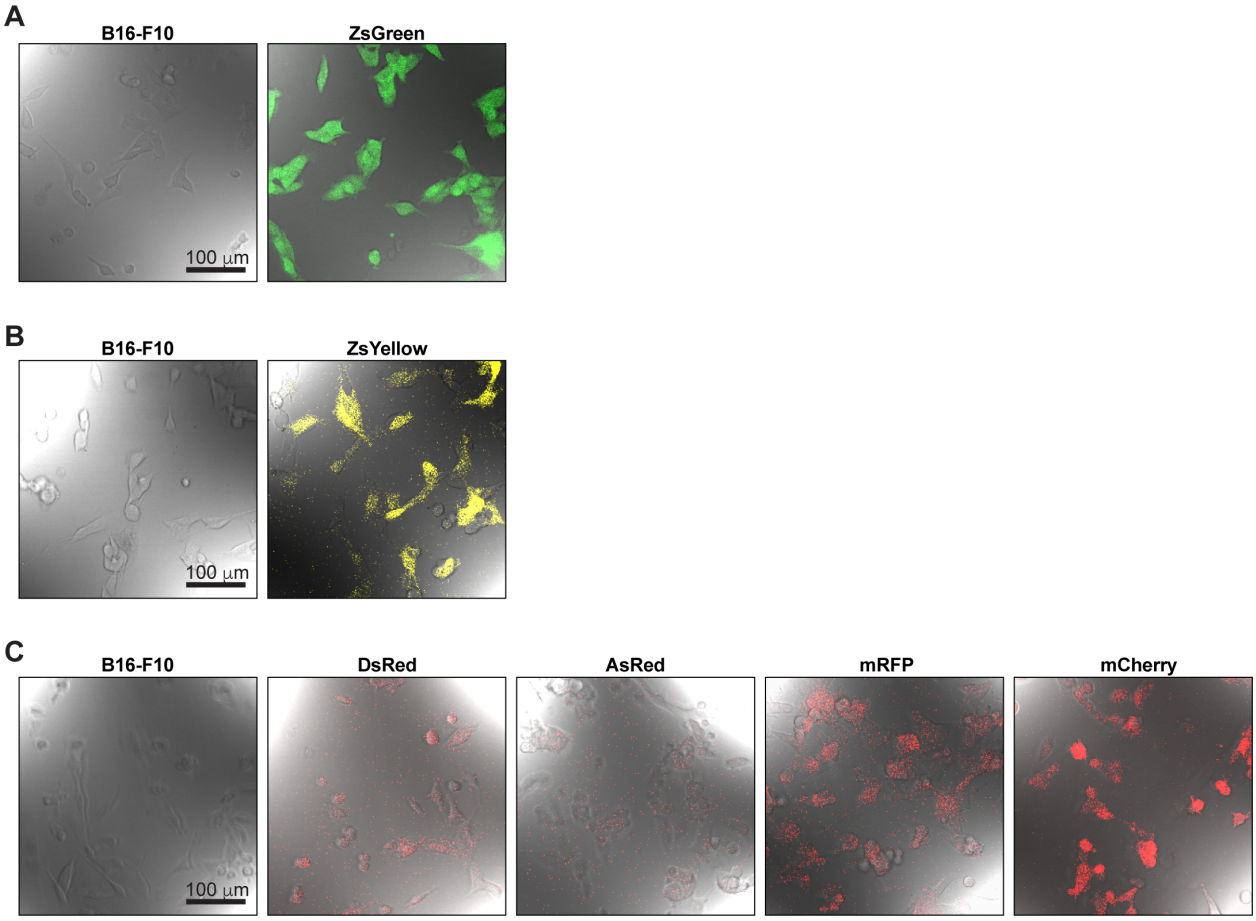

S1 Fig. Similar subcellular localization of fluorescent proteins in FP-expressing B16-F10 cell lines.

Generated B16 melanoma cells with expression of fluorescent protein ZsGreen (**A**), ZsYellow (**B**), AsRed, DsRed, mRFP, and mCherry (all **C**) respectively, overlayed with their bright field images. Images of B16-F10 cell lines were taken to set background fluorescence.

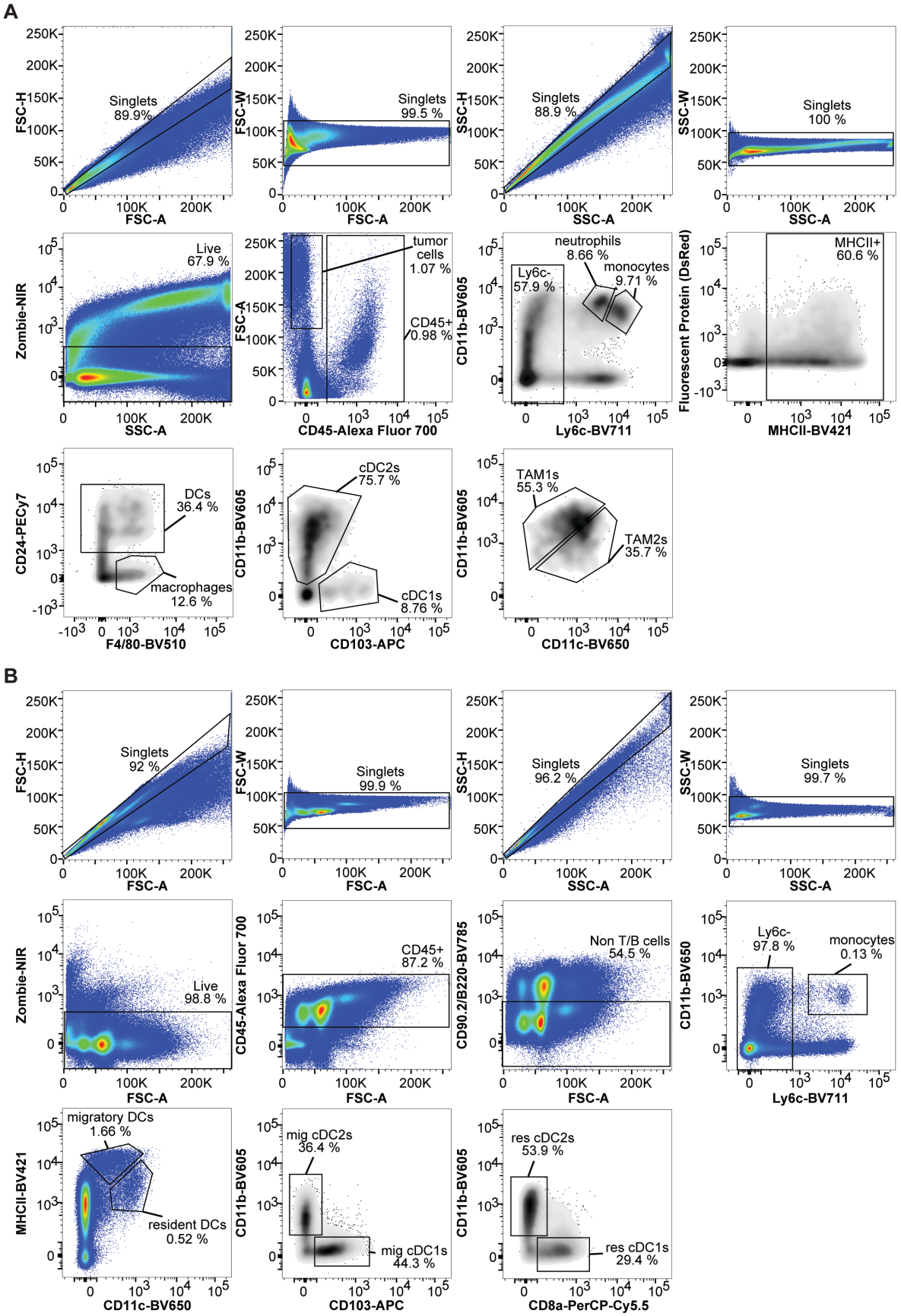
A
Singlets 89.9%
FSC-H
FSC-A
Singlets 99.5 %
FSC-W
Singlets 88.9 %
SSC-H
SSC-A
Singlets 100 %
SSC-W
Live 67.9 %
Zombie-NIR
tumor cells 1.07 %
CD45+ 0.98 %
CD45-Alexa Fluor 700
neutrophils 8.66 %
monocytes 9.71 %
Ly6c- 57.9 %
CD11b-BV605
Ly6c-BV711
MHCII+ 60.6 %
Fluorescent Protein (DsRed)
MHCII-BV421
DCs 36.4 %
macrophages 12.6 %
CD24-PECy7
F4/80-BV510
cDC2s 75.7 %
cDC1s 8.76 %
CD103-APC
TAM1s 55.3 %
TAM2s 35.7 %
CD11c-BV650
B
Singlets 92 %
Singlets 99.9 %
Singlets 96.2 %
Singlets 99.7 %
Live 98.8 %
CD45+ 87.2 %
Non T/B cells 54.5 %
CD90.2/B220-BV785
Ly6c- 97.8 %
monocytes 0.13 %
migratory DCs 1.66 %
resident DCs 0.52 %
mig cDC2s 36.4 %
mig cDC1s 44.3 %
res cDC2s 53.9 %
res cDC1s 29.4 %
CD8a-PerCP-Cy5.5

371

372 **S2 Fig. Gating scheme for flow cytometry analysis of tumor and lymph node samples.**

373 **A)** Cells collected from tumors were analyzed by flow cytometry using the shown gating
374 methods. Percentages of FP positive cells were analyzed in cDC1, cDC2, TAM1, TAM2,
375 monocytes and neutrophils. **B)** Lymph node cells were analyzed using these gating methods. The
376 dump- populations are B220, CD 90.2, NK 1.1 lineage marker negative cells. Percentage of FP
377 positive cells were analyzed in migratory cDC1, migratory cDC2, resident cDC1, resident cDC2
378 and monocytes.

379

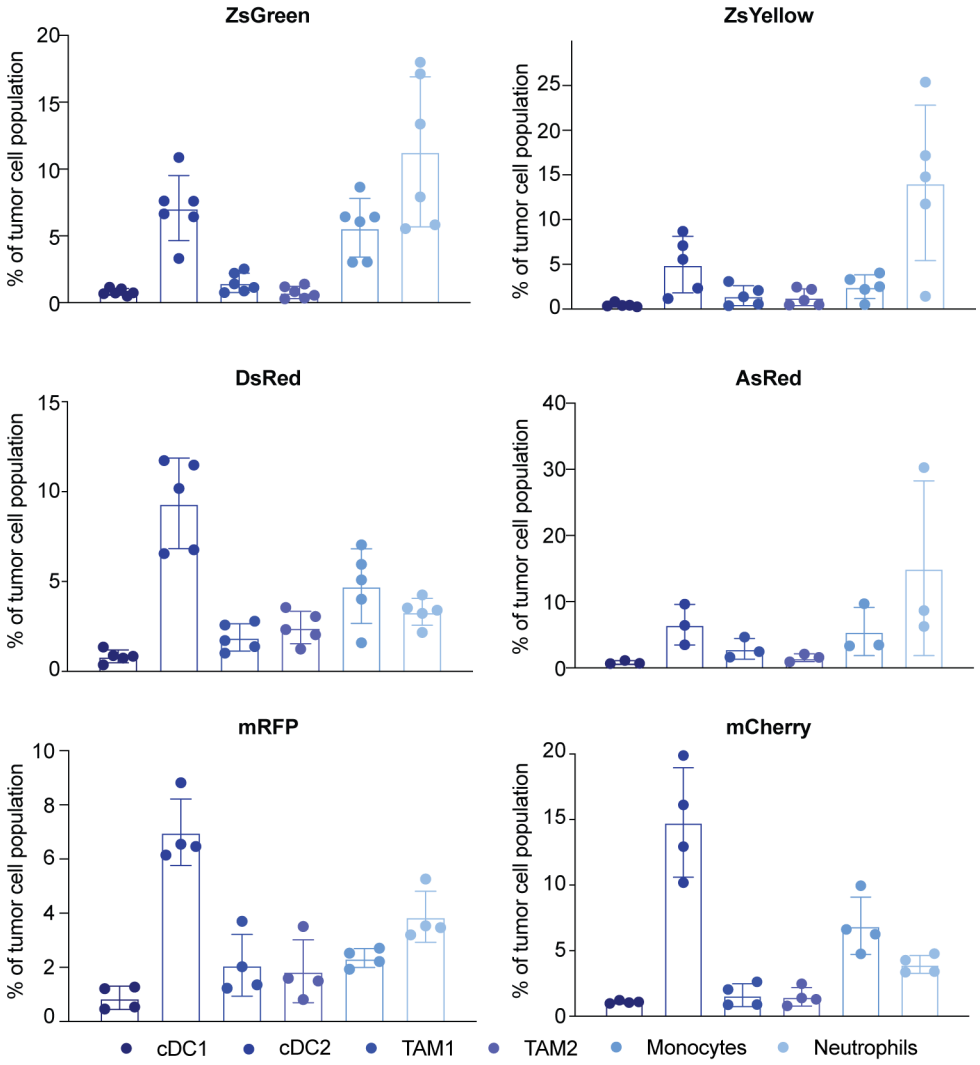

S3 Fig. Tumor cell population distributions.

All tumor cells collected were analyzed for their respective immune cell markers. The cell count for each type of immune cell is then plotted as percentages over the total number of live CD45+ cells.

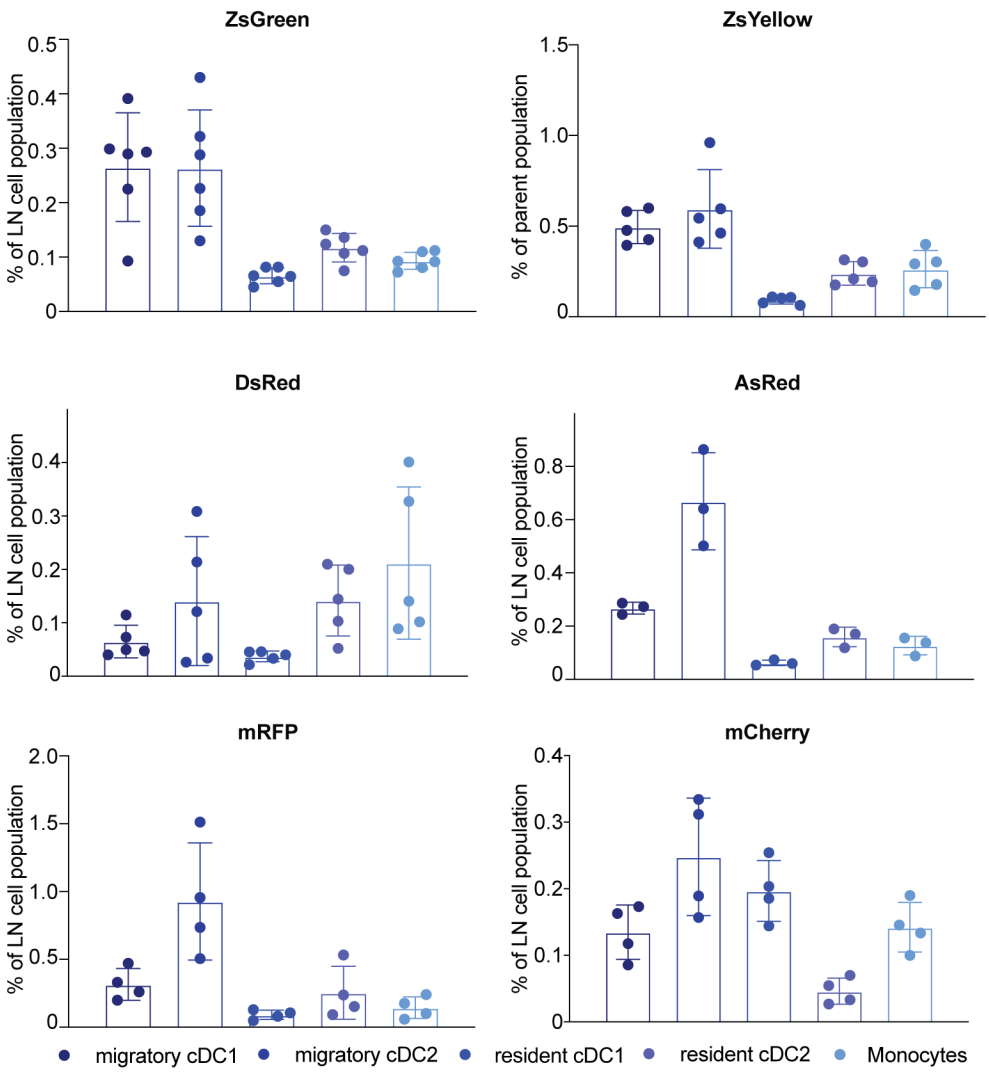

S4 Fig. Lymph node cell population distributions.

All lymph node cells collected were analyzed for their respective immune cell markers. The cell count for each type of immune cell is then plotted as percentages over the total number of live CD45+ cells.